A miniature air breathing direct formic acid fuel cell

S. Ha, B. Adams, R.I. Masel*

Department of Chemical and Biomolecular Engineering, University of Illinois, 600 S Mathews, Urbana, IL 61801, USA

Abstract

Small fuel cells are considered likely replacements for batteries in portable power applications. In this paper, the performance of a 2 cm × 2.4 cm × 1.4 cm passive miniature air breathing direct formic acid fuel cell (DFAFC) at room temperature is reported. The cell produced current density up to 250 mA/cm^2 and power density up to 33 mW/cm^2 at ambient conditions. The fuel cell runs successfully with formic acid concentration ranging from 1.8 and 10 M with little degradation in performance. These results show that passive fuel cells can compete with batteries in portable power applications.
© 2003 Elsevier B.V. All rights reserved.

Keywords: Power density; Passive fuel cells; Batteries

1. Introduction

Recently, there has been considerable interest in the use of miniature fuel cells as replacements for batteries for portable electronics [1]. The advantages of using miniature fuel cells over the conventional batteries are that the miniature fuel cells have a much higher stored energy density, and the ability to do immediate recharge by replacing a fuel cartridge [1]. Most investigators are exploring direct methanol fuel cells (DMFC) for this purpose [6,7], but in this paper we will show that direct formic acid fuel cells (DFAFCs) have considerable advantages over DMFC in portable power applications.

Formic acid is a liquid at room temperature and dilute formic acid is on the US Food and Drug Administration list of food additives that are generally recognized as safe [2]. Formic acid has two orders of magnitude smaller crossover flux through a Nafion® membrane than methanol [3]. This low crossover flux of the formic acid allows one to use the highly concentrated fuel solutions in the DFAFCs [4,5]. The formic acid also has a higher electronic motive force (EMF), as calculated from the Gibbs free energy, than either hydrogen or direct methanol fuel cell [4] and no pumps are needed since formic acid produces CO_2 bubbles that can drive the flow.

In this study, we describe the design and performance of a miniature passive air-breathing DFAFC and show that it can be a useful alternative power source for portable electronic applications.

2. Experimental

The membrane electrode assemblies (MEA) were fabricated in house using a 'direct paint' technique as it is described in elsewhere [4,5]. The active area is 1 cm^2. The 'catalyst inks' were prepared by dispersing the catalyst powders into appropriate amounts of Millipore water and 5% recast Nafion® solution (1100EW, Solution Technology Inc.). Then both the anode and cathode 'catalyst inks' were directly painted onto either side of the Nafion® 117 membrane. A commercially available platinum black (HiSPEC™ 1000 from Johnson Matthey) was used for the cathode catalyst layer at a loading of 12 mg/cm^2. Either platinum black or platinum ruthenium black (HiSPEC™ 6000 from Johnson Matthey) was used for the anode catalyst layer at a loading of 4–12 mg/cm^2. The final catalyst layers contained 10% Nafion® by weight.

An assembly diagram of the miniature air breathing fuel cell is shown in Fig. 1. Both the anode and cathode current collectors were constructed out of titanium foil. In order to protect the titanium from being corroded by the formic acid solutions, they were electrochemically coated with 5 μm of gold. A formic acid reservoir was constructed out of Teflon. The dimensions of the reservoir are 1 cm wide, 1.4 cm high, and 0.56 cm deep. On the top of the reservoir, 100 0.010 in. holes were drilled to vent out the CO_2 gases. Two stainless steel holders were constructed as in Fig. 1. All

* Corresponding author. Tel.: +1-217-333-6841; fax: +1-217-333-5052.
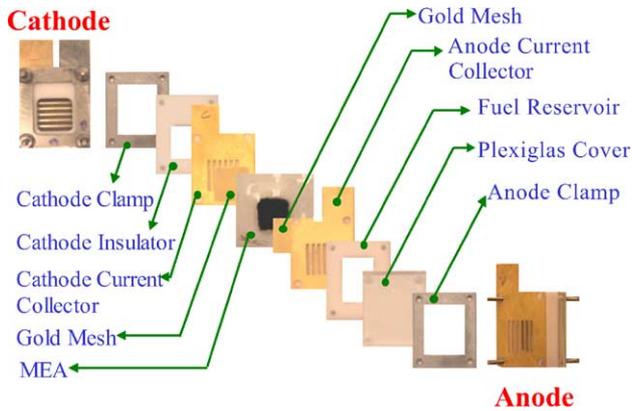*E-mail address:* r-masel@uiuc.edu (R.I. Masel).

Fig. 1. The miniature air breathing direct formic acid fuel cell diagram.

Fig. 2. The cell polarization plot vs. two different anode catalysts: PtBl and PtRuBl. The anode catalyst loading was fixed at $12\,\text{mg/cm}^2$ for both PtBl and PtRuBl. The cathode catalyst was fixed at $12\,\text{mg/cm}^2$ PtBl. The cell was operated with $1.8\,\text{M}$ formic acid and the ambient air at the room temperature.

of the components of the miniature fuel cell that are shown in Fig. 1 are put together using bolts and nuts on the four corners of the miniature fuel cell.

We tested our miniature fuel cell with and without the presence of the carbon cloth on the anode side. We also varied the type of the carbon cloth that we used on the anode side. We used three different types of the carbon cloth. They are an ETEK ELAT V2 single sided diffuser, ETEK plain carbon cloth type A, and oxygen plasma treated carbon cloth. We also tested the cell with and without $1\,\text{cm} \times 1\,\text{cm}$ pieces of Alpha Aesar #40931 gold mesh on both sides of the MEA. The gold mesh was placed between the current collector and the MEA on both the anode and cathode sides as it is shown in Fig. 1.

Both cell polarization curves and constant voltage tests were acquired using a fuel cell testing station (Fuel Cell Technologies Inc.). Double distilled 88% formic acid (GFS) was diluted with the Millipore water to give a final concentration ranging from 1.8 to 13.2 M. The formic acid was injected into the fuel reservoir using a micro syringe. The cathode was opened to air. No carbon cloth was used on the cathode for this paper. The membrane was used without any prior conditioning.

3. Results

Fig. 2 shows the performance of our fuel cell in $1.8\,\text{M}$ formic acid using either platinum black or platinum ruthenium (PtRu) as the anode catalyst. In either case an open cell potential (OCP) of nearly $800\,\text{mV}$ is observed. The potential goes down as current is drawn from the cell, and interestingly the performance is better on the reverse scan. At low cell potential, PtBl catalyst gives a higher current density than the PtRuBl catalyst. However, in overall cell performance, there is relatively little difference between the two anode catalysts. Fig. 3 shows the effect of two different anode catalyst loadings on the cell performance. Notice that the anode catalyst loading has very little effect on the fuel cell performance between 4 and $12\,\text{mg/cm}^2$.
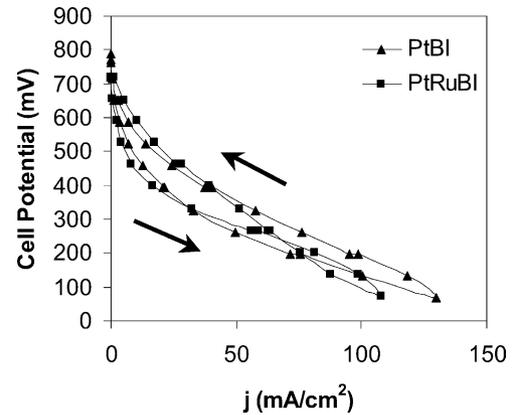
Fig. 4 shows the effect of the different types of the anode carbon cloth on the cell polarization profile. We used three different types of the anode carbon cloth, and they are the carbon cloth with no Teflon layer (plain carbon cloth), carbon cloth with a single side Teflon layer (Teflon carbon cloth), and oxygen plasma treated carbon cloth (modified carbon cloth). In Fig. 4, the miniature cell is also tested with no carbon cloth for a comparison. According to Fig. 4, the miniature cell with no carbon cloth generates the highest current density over the entire cell potential range. The miniature cell with the modified carbon cloth generates a similar current density as the cell with no carbon cloth, which indicates that the modified carbon cloth does not impose any significant formic acid mass transport limitation. For the miniature cell with the plain carbon cloth, the current density curve drops sharply from its OCP value and generates less than $10\,\text{mA/cm}^2$ of current density. The
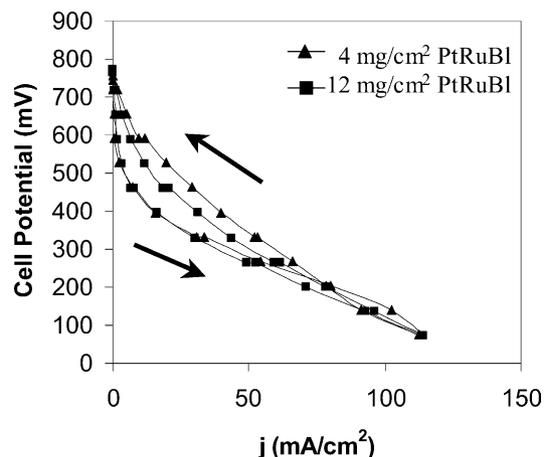

Fig. 3. The cell polarization plot vs. two different anode catalyst loadings: 4 and $12\,\text{mg/cm}^2$ PtRuBl. The cathode catalyst was fixed at $12\,\text{mg/cm}^2$ of PtBl. The cell was operated with $1.8\,\text{M}$ formic acid and the ambient air at the room temperature.
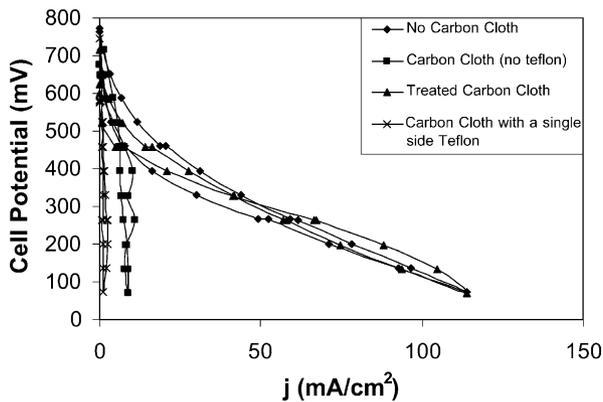
Fig. 4. The cell polarization plot vs. the different anode wicking materials. Anode was 4–12 mg/cm^2 PtRuBl and cathode was 12 mg/cm^2 PtBl. The cell was operated with 5 M formic acid and the ambient air at the room temperature.

miniature cell with the Teflon carbon cloth generates less than 2 mA/cm^2 of current density due to the high mass transport limitation of the formic acid through the hydrophobic layer of Teflon. According to Fig. 4, the cell with no carbon cloth gives the highest OCP while the cell with the Teflon carbon cloth gives the lowest OCP.

Fig. 5A shows the effect of the different formic acid concentration on the cell polarization curve profile. The cell polarization curves were acquired by using the formic acid concentration ranging from 1.8 to 13.2 M. For these tests, no carbon cloth was used on the anode or cathode. Above a cell potential of 200 mV, the current densities slightly decrease as the formic acid concentration increases from 1.8 to 8.8 M. Below 200 mV, the current densities are very similar for the same concentration range. From Fig. 5A, 113 mA/cm^2 is the maximum current density at room temperature. At 13.2 M formic acid, the current density decreases sharply over the entire cell potential range. A key feature to note from Fig. 5 is the high operational concentration range for our miniature air breathing DFAFC. As seen from the cell polarization curves in Fig. 5A, the miniature cell can operate without a major performance drop in the formic acid concentration between 1.8 and 8.8 M.

In Fig. 5B, the results from Fig. 5A are plotted in terms of power density for the different formic acid concentration. Between the formic acid concentration of 1.8 and 8.8 M, the power density plots are twisted at around 75 mA/cm^2. A further study is needed to understand these twisting behaviors. Because of these twistings, at the fuel concentration between 4.4 and 8.8 M, the maximum power density occurs at two different current density points. From Fig. 5B, the maximum power density of 16.6 mW/cm^2 is observed at the formic acid concentration of 1.8 and 4.4 M.

Fig. 6 shows the effects of the different formic acid concentration on the apparent OCP of our miniature fuel cell. At formic acid concentration of 1.8 M, a maximum OCP of 0.756 V is observed. As the formic acid concentration increases from 1.8 to 13.2 M, the OCP of the cell decreases.
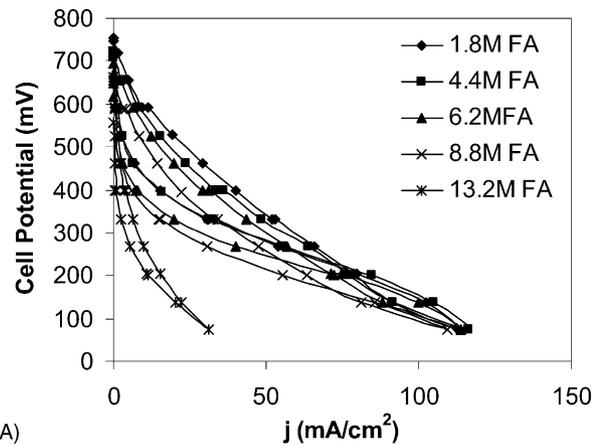
(A)
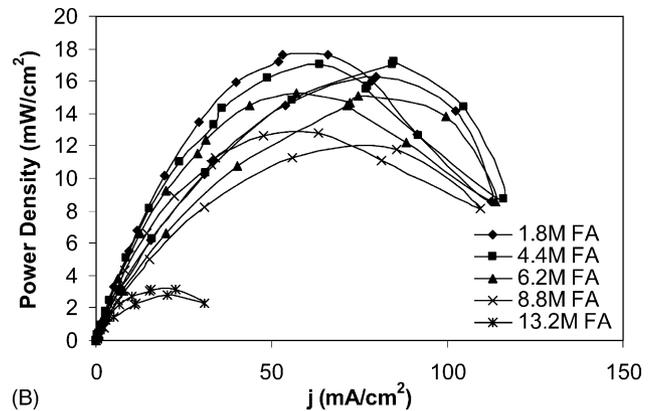
(B)

Fig. 5. Formic acid/ambient air current density vs. the formic acid concentration at the room temperature. (A) Cell potential and (B) power density curves. Anode was 12 mg/cm^2 PtRuBl and cathode was 12 mg/cm^2 PtBl. The ambient air was used as oxidant.

The changing of the formic acid concentration from 1.8 to 13.2 M causes the OCP to drop nearly 200 mV. Fig. 6 also shows the high frequency cell resistance. The cell resistance is not influenced much by the formic acid concentration changing from 1.8 to 8.8 M, while the OCP of the cell decreases by 93 mV for the same concentration change. As the
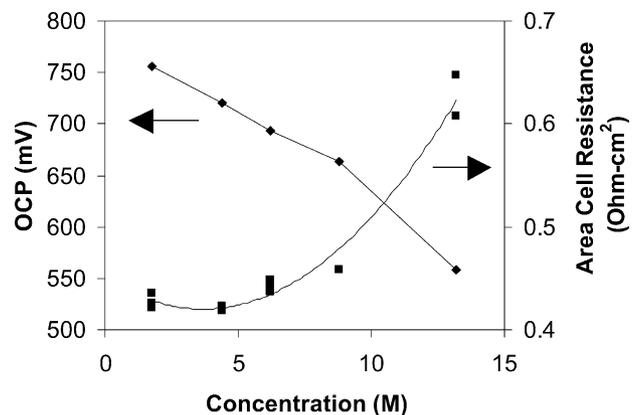

Fig. 6. Plot of formic acid concentration vs. OCP (left Y-axis) and area cell resistance (right Y-axis) for the cell at the room temperature. The ambient air was used.
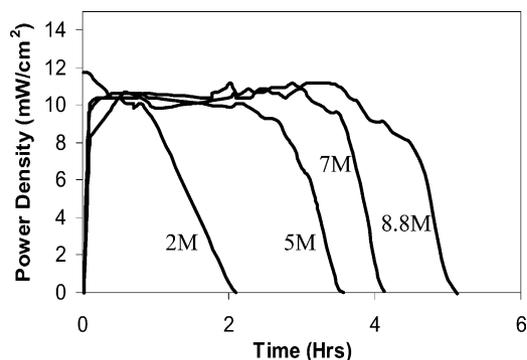
Fig. 7. Plot of constant cell potential test vs. different formic acid concentration at the room temperature. The cell potential was fixed at 0.26 V. The ambient air was used.

formic acid concentration increases from 8.8 to 13.2 M, the cell resistance increases significantly while the OCP of the cell drops further more.

In Fig. 7, the constant cell voltage tests are reported with various formic acid concentrations. For these tests, no carbon cloth was used on the anode or cathode. The voltage of the miniature cell was set constant at 0.26 V. At 2 M formic acid, the power density increases initially as the operation time increases. However, as soon as it reaches the maximum power density after a short while, its power density output drops. After 2 h of operation, its power output at 0.26 V goes down to zero when all of the fuel is used. Between the fuel concentration of 5 and 8.8 M, the power densities initially increase until they reach the steady state. In Fig. 7, the operation time is proportional to the fuel concentration. As the fuel concentration increases, the cell operation time at 0.26 V increases too. At the fuel concentration of 8.8 M, the miniature fuel cell generates 10 to 11 mW/cm^2 of the power density up to 4 h.

Fig. 8 shows the effect of the cell potential on its operation time. For this test, no carbon cloth was used on the anode or cathode. In Fig. 8, the constant cell voltage tests were conducted at 0.26 and 0.46 V with 5 M formic acid. The average power density output is about 10 and 6.6 mW/cm^2 at
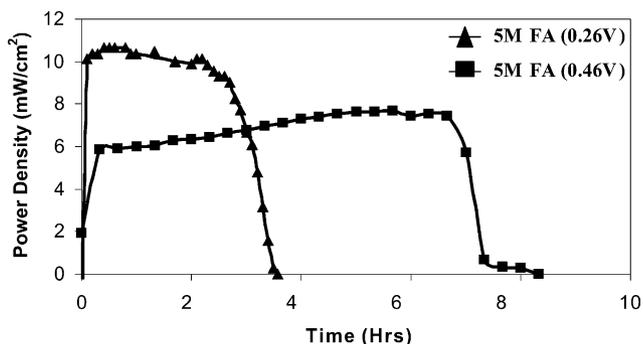

Fig. 8. Plot of constant cell potential tests at two different cell potential values. The cell potential was fixed at 0.26 and 0.46 V in each test. The cell was operated with 5 M formic acid and the ambient air at the room temperature.

0.26 and 0.46 V, respectively. By integrating the areas under the curves in Fig. 8, we calculate the total energy generation for the cell operating at each voltage. The cell operating at 0.26 V produces a total of 113 J, and the cell operating at 0.46 V produces 151 V. A keynote here is that the cell operating at a higher voltage generates a greater total energy, and works more efficiently. Fig. 9 shows the results of a run where pieces of gold mesh were inserted between the current collector and the MEA on both sides of the MEA. In this case the maximum power increases to 33 mW/cm^2 and the maximum current increases to 250 mA/cm^2.

4. Discussion

The results here provide further evidence that DFAFCs are quite attractive for portable power applications. The results in Fig. 9 show that passive devices running at ambient conditions (20 °C) produce 33 mW/cm^2. By comparison Chang et al. [6] reports that his passive DMFC produced about 5 mW/cm^2 under conditions similar to those reported here and 10 mW/cm^2 when the cathodes were modified appropriately. Blum et al. [7] report that their passive DMFC produced 12.5 mW/cm^2 with continuous recharge. Clearly, our passive DFAFC competes quite well with other's passive DMFC in terms of power output.

Our DFAFC also compares well with DMFC in terms of fuel power density. The direct formic acid fuel cell reported here runs successfully with 10 M solutions as it was shown in Fig. 9. By comparison, Chang found that his DMFC ran poorly at methanol concentrations above 2 M. While neat formic acid has a lower theoretical energy density than neat methanol (2086 Wh/l for formic acid versus 4690 Wh/l for methanol), a 10 M formic acid solution has a higher energy density than a 2 M methanol solution (787 Wh/l for 10 M formic acid versus 380 Wh/l for 2 M methanol).

Finally, OCP of the fuel cell is quite reasonable. The passive cell in Fig. 5 shows an OCP of 756 mV with about 2 M formic acid. By comparison Chang reports an OCP for a passive DMFC below 700 mV, while Scott et al. [8] report an OCP of 640 mV for the DMFC at 363 K with a compressed air at 2 bar and a forced feed of 2 M methanol. Overall, the passive DFAFC shows a quite good performance compared to a passive DMFC, and dilute formic acid is edible and generally recognized as safe [2].

There are some surprises in the data. First the cell performance was relatively insensitive to the fuel concentration (Fig. 5(A)), the anode catalyst composition (Fig. 2), or the anode catalyst loading (Fig. 3). Gold mesh on the anode improved the fuel cell performance (Fig. 9). Yet the addition of the plain or Teflon coated carbon cloth on the anode significantly reduced the fuel cell performance (Fig. 4). The fuel cell operated well on 10 M formic acid (Fig. 9), but performed poorly on 13.2 M formic acid. By comparison, Rice et al. [4,5] found that an actively pumped DFAFC shows that performance depends on the catalyst composition and the
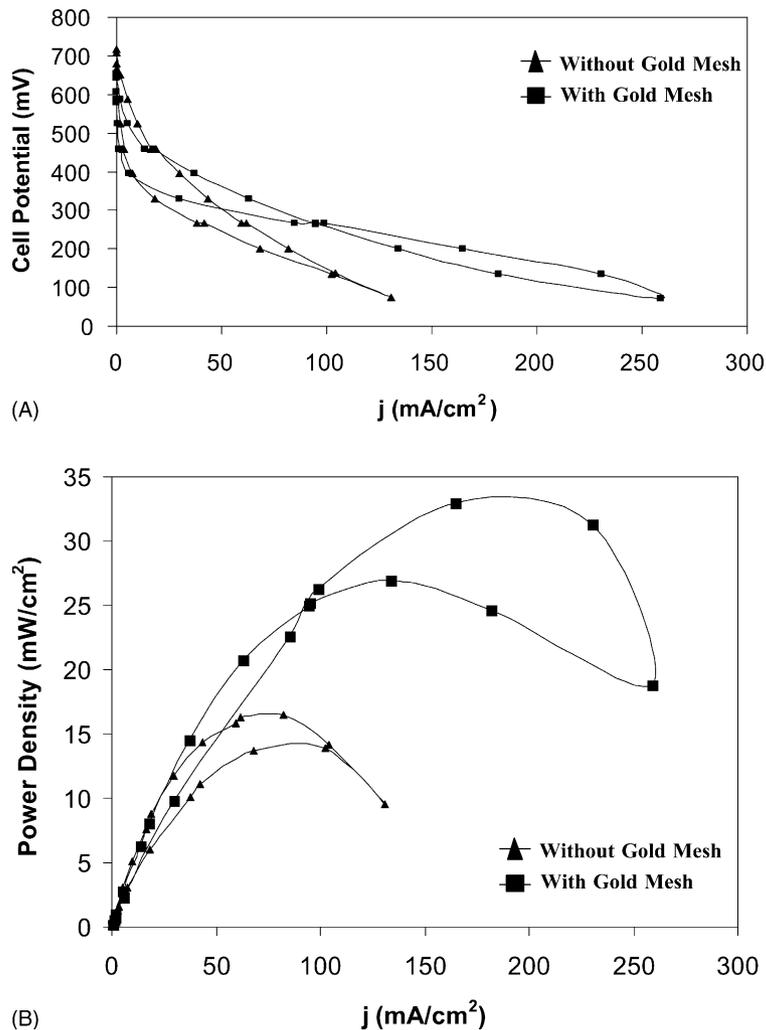
Fig. 9. Effect of gold meshes on the cell performance at the room temperature. (A) Cell potential and (B) power density curves. The anode was 4 mg/cm^2 PtRuBl and the cathode was 12 mg/cm^2 PtBl. 6 M formic acid was used for the cell without gold meshes and 10 M formic acid was used for the cell with gold meshes. The ambient air was used for both cells.

fuel concentration. While Teflon coated carbon cloth reduced the performance of the actively pumped cells, plain carbon cloth seemed to have no significant effect on the cell performance [4,5]. The actively pumped cells worked at formic acid concentrations up to 20 M. Also the open cell potential was about 0.1 V higher in the actively pumped cells than in the passive cells. Evidently, there are some significant differences between the performance of the passive DFAFCs and actively pumped DFAFCs that need to be explained.

We believe that the absence of water management in the passive cells lead them to have slightly reduced performance compared to the active cells. Recall that humidified air or oxygen was used in the experiments with the actively pumped cells [4,5], while dry air was used in the experiments with the passive cells. Also there was no carbon cloth on the membranes in the passive cells (Fig. 5), while carbon cloth was used in the active cells [4,5]. Thus, one would expect the membranes in the passive cells to be less hydrated than the membranes in the active cells.

Fig. 6 shows that the cell resistance of the passive cell is similar to that of the active cell at formic acid concentrations below 10 M. However, the cell resistance suddenly rises if 13 M (51% formic acid, 49% water) solutions are used. By comparison, in the actively pumped cells, the cell resistance slowly rose as the formic acid concentration increased, but with 20 M solutions, the cell resistance was still below 0.6 Ω cm. Evidently, more water is needed in the fuel with the passive cells than with the active cells.

Our suggestion, therefore, is that the membrane is not being adequately hydrated when the passive cells are run with fuel solutions containing high formic acid concentrations and correspondingly low water concentrations. With the current design, we are limited to 13 M solutions. In order to increase the working formic acid concentration higher than 13 M, water management seems to be a key issue in passive fuel cell design.

It also appears that mass transfer/diffusion effects are more important in the passive fuel cells than in the actively

Table 1
The contact angles of the formic acid with the different types of the carbon cloth and their respective fuel cell power density at 0.26 V

	The contact angle ($^\circ$)	The power density at 0.26 V (mW/cm^2)
A modified carbon cloth (with oxygen plasma)	0	18
A plain carbon cloth	135	3
A Teflon coated carbon cloth	155	0.5

The values of the power density are obtained from Fig. 4.

pumped cells [4,5]. We find that the plain carbon cloth reduces the performance of the passive cell dramatically as it is shown in Fig. 4. We believe that the presence of the plain carbon cloth imposes such reduction in our passive fuel cell's performance, because it is hydrophobic and the formic acid does not wet its surface well due to a high surface tension. On the other hand, the presence of the plasma modified carbon cloth did not show any performance reduction as it is shown in Fig. 4. The modified carbon cloth in our passive DFAFC works well because the oxygen plasma makes the carbon cloth hydrophilic [7], hence the formic acid solution is easily adsorbed into the plasma modified carbon cloth. One might have expected Teflon coated carbon cloths to reduce the fuel cell's performance the most extensively, since the Teflon is very hydrophobic and the formic acid solution does not wet it. A contact angle indicates a wettability of a liquid on a solid surface. The contact angle is zero if the liquid wets the solid surface fully, and it increases as the surface tension between the liquid and solid increases. Table 1 shows the relationship between the contact angles of the formic acid with the different types of the anode carbon cloth and the cell power density at 0.26 V. According to Table 1, the modified carbon cloth gives the contact angle of zero and the highest power density. The Teflon coated carbon cloth gives the highest contact angle of 155° and the lowest power density as we are expected.

Fig. 9 shows that using the gold mesh on both the anode and cathode sides increase the passive DFAFC performance. We believe that the presences of the gold mesh increase the performance of the cell by enhancing the electron flow, since the gold is a good electron conductor.

5. Conclusion

The miniature air breathing DFAFC was constructed and its performances were tested. Figs. 5A and 7A show that our miniature air breathing fuel cell using formic acid as its fuel is a good alternative power source, which can replace the conventional battery for the small electronic devices in the future. Our miniature DFAFC can be operated at a much higher fuel concentration range than a typical DMFC. Our miniature cell, at 8.8 M formic acid, produced the maximum current and power density of 107 mA/cm^2 and 12.2 mW/cm^2, respectively. The OCP of our miniature cell decreased as the formic acid concentration increased. We speculate that both the dehydration of the membrane and the fuel crossover caused our cell's OCP drop. Despite of this drop of the OCP at the higher formic acid concentration, our miniature cell at 8.8 M formic acid had 663 mV of the OCP, which is about the best OCP value the DMFC can give at a much lower fuel concentration. Dehydration of the membrane becomes a major issue at higher formic acid concentration, as seen by the increase in cell resistance, causing an overall decrease in cell performance. From the presented experimental results in this paper, the dehydration of the membrane started to affect the overall cell performance significantly at the formic acid concentration between 8.8 and 13.2 M and higher.

We are only at the beginning stage of studying miniature air breathing direct formic acid fuel cell. Our miniature cell has to be further optimized to enhance cell performance in the future. We need to optimize the catalyst loading and the Nafion$^\circledR$ content within the catalyst layer. A water management of the passive DFAFC would be also important. In order to increase the working fuel concentration, we need to develop a novel method to prevent the Nafion$^\circledR$ membrane from dehydrating when the high concentration formic acid is used. For the future research, we also need to consider how to remove the byproduct water from the cathode before it limits the oxygen transport.

References

[1] B.J. Feder, New York Times, 16 March 2003.
[2] US Code of Federal Regulations, 21 CFR 186.1316, 21 CFR 172.515.
[3] Y.-W. Rhee, S. Ha, R.I. Masel, J. Power Sources 117 (2003) 35–38.
[4] C. Rice, S. Ha, R.I. Masel, P. Waszczuk, A. Wieckowski, T. Barnard, J. Power Sources 111 (2002) 83.
[5] C. Rice, S. Ha, R.I. Masel, A. Wieckowski, J. Power Sources 115 (2003) 229.
[6] H. Chang, J.R. Kim, J.H. Cho, H.K. Kim, H.K. Choi, Solid State Ionics 148 (2002) 610.
[7] A. Blum, T. Duvdevani, M. Philosoph, N. Rudoy, E. Peled, J. Power Sources 117 (2003) 22–25.
[8] K. Scott, W.M. Taama, P. Argyropoulos, K. Sundmacher, J. Power Sources 83 (1999) 204–216.